

Electronic properties of $\text{LaNi}_{4.75}\text{Sn}_{0.25}$, $\text{LaNi}_{4.5}\text{M}_{0.5}$ (M=Si, Ge, Sn), $\text{LaNi}_{4.5}\text{Sn}_{0.5}\text{H}_5$

J.-C. Crivello, M. Gupta*

E.A. 3547, Bâtiment 415, Science des Matériaux, Université Paris-Sud, 91405 Orsay, France

Received 1 October 2002; accepted 25 October 2002

Abstract

The effect of Ni substitutions by group IVA (Si, Ge, Sn) s-p elements on the electronic properties of LaNi_5 and its hydrides has been studied using ab initio band structure calculations for several substitution rates. The site and angular momentum analysis of the densities of states (DOSs) are used to discuss the factors that affect the electronic structure, the bonding and stability of the substituted intermetallic compounds and their corresponding hydrides. Our results are discussed in light of available experimental data and previous theoretical work.

© 2002 Elsevier B.V. All rights reserved.

Keywords: Hydrogen storage materials, AB_5 , Sn, intermetallic; Electronic band structure

1. Introduction

Substitutions at the La and Ni sites have been widely used to modify the thermodynamic properties of LaNi_5 and play a crucial role in the selection of the alloy for specific technological applications, since they affect the stability and the maximum hydrogen content [1–3]. Substitution at nickel sites by s-p elements of group IIIA (such as Al) and group IVA (Si, Ge, Sn) are known to lower the pressure plateaux of the isotherms [4–8]. In addition, substitutions by the group IVA elements, in particular by Sn, improve the cycling lifetimes of the hydrides both in the gas phase and in nickel–metal hydride batteries [9,10].

In this paper, we present an investigation of the electronic structure of several intermetallic compounds $\text{LaNi}_{5-x}\text{M}_x$ ($x=0.25, 0.5$; M=Si, Ge, Sn) using ab initio band structure calculations. The effect of the substituting elements on the chemical interactions and on band filling are discussed in relation with experimental data and previous theoretical work on Ni substitutions by other s-p elements such as Al and an s element of the 3d series, Cu [11,12].

We have also investigated the electronic properties of the hydrides ($\text{LaNi}_{5-x}\text{Sn}_x\text{H}_5$, $x=0.5$). An analysis of the factors that control the stability of the compounds is presented.

2. Crystallographic data

LaNi_5 is known to be described in the $P6/mmm$ space group with atoms La and Ni occupying, respectively, the $1a$, $2c$ and $3g$ Wyckoff sites. Structural data [13–15] show that substitutions of the nickel atoms by IVA elements occur at the $3g$ site as shown in Fig. 1. Lattice parameters determined by X-ray and neutron diffraction studies are summarized in Table 1.

Several types of interstitial hydrogen sites are available in this structure. The neutron diffraction analysis [17,13] give similar deuterium site occupancy in LaNi_5D_5 and $\text{LaNi}_{4.5}\text{Sn}_{0.5}\text{D}_5$ as shown in Table 2. In the present calculation, we have ordered the H atoms at three tetrahedral sites (Ni_4 , La_2Ni_2 , LaNi_3) and an octahedral site (La_2Ni_4), we doubled the unit cell along \vec{c} axis as shown in Fig. 1 to study the $\text{LaNi}_{4.5}\text{M}_{0.5}$ compounds, and we used integer instead of fractional occupancies of the D sites as indicated in Table 2.

*Corresponding author.

E-mail address: michele.gupta@scmat.u-psud.fr (M. Gupta).

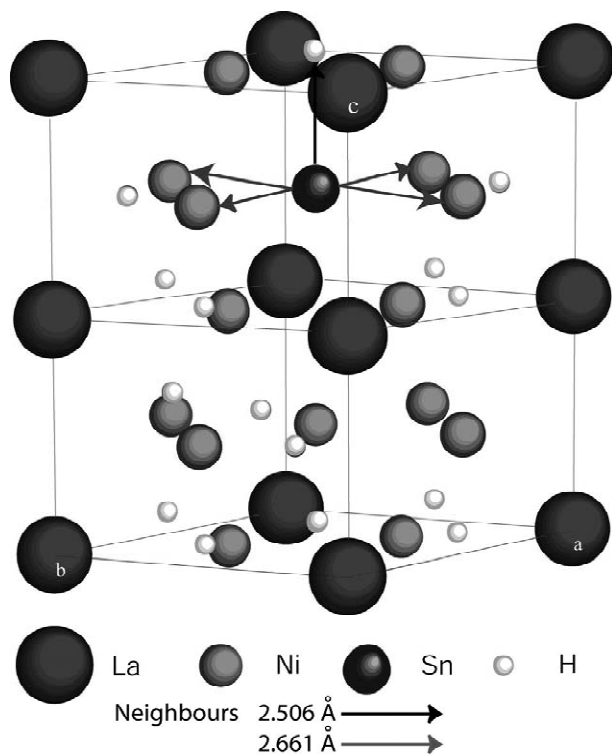


Fig. 1. The model unit cell used for $\text{LaNi}_{4.5}\text{Sn}_{0.5}\text{H}_5$ (two formula units).

Table 1
Experimental values of the lattice parameters of $\text{LaNi}_{5-x}\text{M}_x\text{H}_y$ ($\text{M}=\text{Si}$, Ge , Sn)

	a (Å)	c (Å)	V (Å ³)	c/a	$\Delta V/V$	Ref.
LaNi_5	5.006	3.993	86.75	0.798	–	[8]
$\text{LaNi}_{4.5}\text{Si}_{0.5}$	5.007	3.992	86.67	0.797	–0.09	[14]
$\text{LaNi}_{4.6}\text{Si}_{0.4}$	5.023	3.995	87.26	0.795	0.59	[8]
$\text{LaNi}_{4.5}\text{Ge}_{0.5}$			88.32		1.81	[6]
$\text{LaNi}_{4.75}\text{Sn}_{0.25}$	5.056	4.028	89.18	0.797	2.80	[16]
$\text{LaNi}_{4.5}\text{Sn}_{0.5}$	5.104	4.074	91.92	0.798	5.96	[13]
LaNi_5D_5	5.395	4.242	106.93	0.786	23.26	[17]
$\text{LaNi}_{4.5}\text{Sn}_{0.5}\text{D}_{5.2}$	5.390	4.317	108.6	0.801	25.19	[13]

3. Computational method

The band structure calculations have been performed using the density functional theory (DFT) in the local

density approximation (LDA). We have used the self-consistent linear muffin-tin orbital method (LMTO) within the atomic sphere approximation (ASA) [18]. The von Barth-Hedin approach was used to determine the exchange and correlation terms of the crystal potential.

Scalar relativistic corrections were taken into account, but spin-orbit coupling was ignored. Angular momentum values up to $l=3$ at the metal sites and $l=1$ at the H site were included.

We sampled the irreducible Brillouin zone with 315 \vec{k} -points and calculated the density of states (DOS) with the linear energy tetrahedron method in a mesh of 1-mRy. The origin of the energy scale is located at the Fermi energy E_F .

4. Results and discussion

4.1. Electronic structure of the intermetallic compounds $\text{LaNi}_{5-x}\text{M}_x$ ($\text{M}=\text{Si}$, Ge , Sn and $x=0, 0.25, 0.5$)

Previous investigations of the electronic structure of LaNi_5 based Haucke compounds and some of their hydrides [19,20] have shown that the occupied states of the valence band are mainly composed of Ni-3d states hybridized with La-5d states. In the intermetallic, the Ni-3d bands are not filled and the Fermi level falls below the valley separating the bonding Ni–La high DOS peak from the empty antibonding La–Ni structure.

The total DOSs of the tin substituted compounds $\text{LaNi}_{5-x}\text{Sn}_x$ ($x=0.25, 0.5$), obtained, respectively, with a quadruple and double unit cell, are plotted in Figs. 2 and 3; the site and partial wave analysis of the DOS of $\text{LaNi}_{4.5}\text{Sn}_{0.5}$ is presented in Fig. 4. Above the 5p states of lanthanum, very localized at 16.5 eV below E_F , we observe in the tin substituted compounds, a new structure located around -9 eV corresponding to the 5s states of Sn.

The Sn-5p states are located at higher energies, above -7 eV where they interact with the conduction metal-d bands and to a lesser extent with metal s-p states. In Fig. 4, we see a substantial bonding interaction of the Sn-p with La and Ni states as well as a smaller but non-negligible contribution of Sn-s interaction with the Ni-d states of its

Table 2
Site occupancy of deuterium in $\text{LaNi}_{5-x}\text{M}_x\text{D}_{5-x}$ ($\text{M}=\text{Sn}$ and $x=0.0, 0.5$) from neutron diffraction data and model used for the calculation

	Tetrahedral Ni_4	Tetrahedral La_2Ni_2	Tetrahedral LaNi_3	Octahedral La_2Ni_4	Space group/ Ref.
$\text{LaNi}_5\text{D}_{5.0}$	$2b$ ($1/3, 2/3, z=0.80$) 0.20	$6c$ ($x=0.146, 2x, z=0.25$) 1.78	$6c$ ($x=0.225, 2x, z=0.33$) 0.68	$12d$ ($x=0.480, 0, z=0.04$) 2.34	$P63mc$ [17]
$\text{LaNi}_{4.5}\text{Sn}_{0.5}\text{D}_{5.2}$	$4h$ ($1/3, 2/3, z=0.38$) 0.21	$6m$ ($x=0.14, 2x, 1/2$) 1.78	$12o$ ($x=0.21, 2x, z=0.33$) 0.56	$12n$ ($x=0.47, 0, z=0.11$) 2.61	$P6/mmm$ [13]
$\text{LaNi}_{5-x}\text{Sn}_x\text{H}_5$ model	0	2	0.5	2.5	

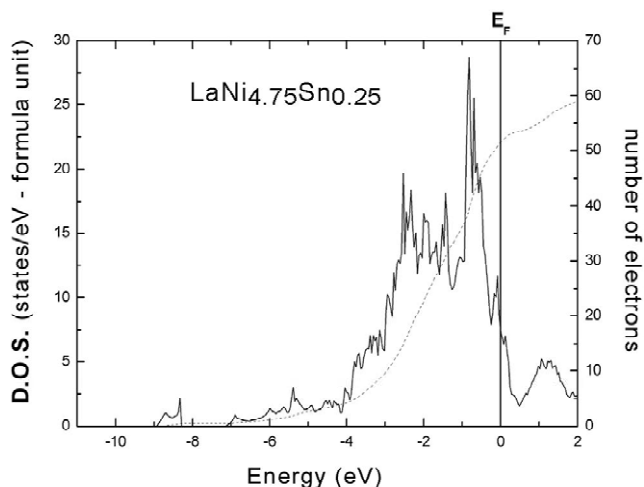


Fig. 2. Total density of states (full line, left hand side scale) and number of electrons (dashed line, right hand side scale) of $\text{LaNi}_{4.75}\text{Sn}_{0.25}$.

four nearest neighbors (occupying the $3g$ sites at $z=3/4$), and with the La-d orbitals. This chemical bonding interactions of Sn with La and Ni can play a role in preventing metal diffusion and improving the cycling life time of the intermetallic observed experimentally [9,10].

In the tin substituted intermetallics, the Ni-d bands are not entirely filled, however, as a function of increasing tin concentration, the number of holes the Ni-d bands decreases. Similar trend has been observed upon substitution of Ni by an s element of this 3d series, Cu, while the substitution of Ni by Al leads to a complete filling of the Ni-d bands [11,12].

In $\text{LaNi}_{5-x}\text{Sn}_x$, the DOS at E_F is dominated by the contribution of the Ni-d states, its value decreases progressively with increasing values of x , from 0.0 to 0.5.

The very localized La-4f states, plotted in Fig. 3 are empty and located around 3 eV above E_F .

The total DOSs of Si and Ge substituted $\text{LaNi}_{4.5}\text{M}_{0.5}$

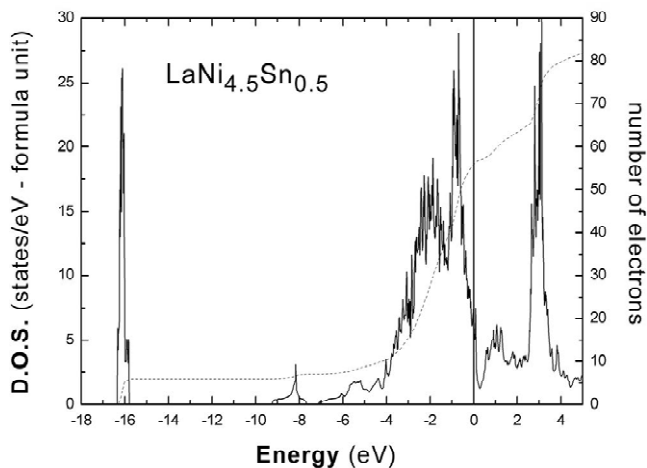


Fig. 3. Total density of states (full line, left hand side scale) and number of electrons (dashed line, right hand side scale) of $\text{LaNi}_{4.5}\text{Sn}_{0.5}$.

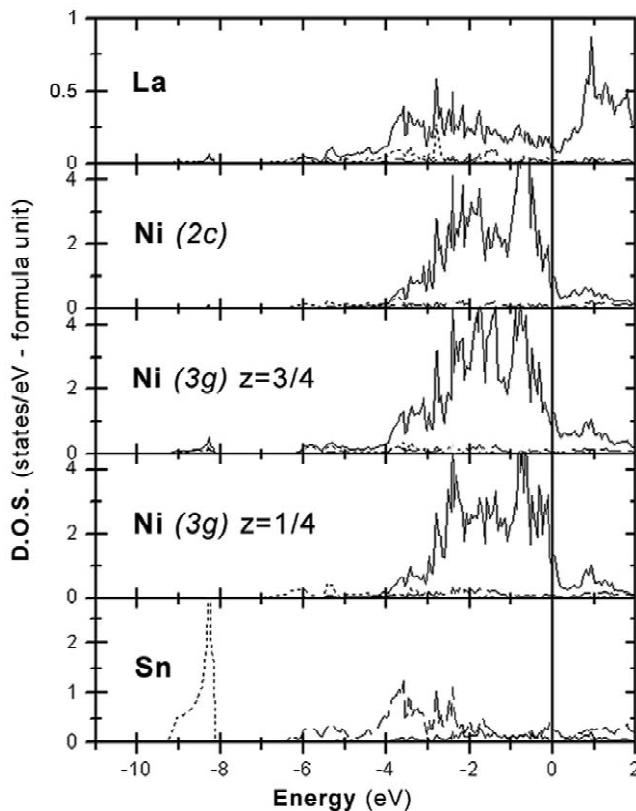


Fig. 4. Partial wave analysis of density of states (DOS) of $\text{LaNi}_{4.5}\text{Sn}_{0.5}$ around the atomic sites (d states: full line, p states: dashed line, s states: dotted line).

intermetallic are presented in Fig. 5. The features are similar to those discussed for $\text{LaNi}_{4.5}\text{Sn}_{0.5}$, in particular the Ni-d band incomplete filling. However, we observe small differences associated to the relative positions and spatial extension of the IVA elements s-p states; moreover the volume increase from Si to Ge and Sn results in a narrowing of Ni-d bands.

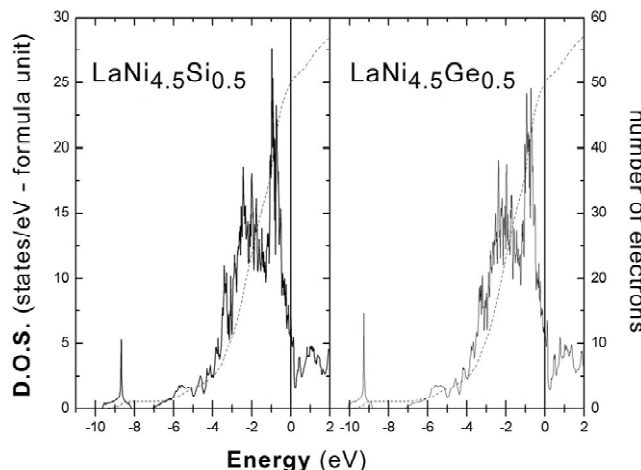


Fig. 5. Total density of states (full line, left hand side scale) and number of electrons (dashed line, right hand side scale) of $\text{LaNi}_{4.5}\text{Si}_{0.5}$ and $\text{LaNi}_{4.5}\text{Ge}_{0.5}$.

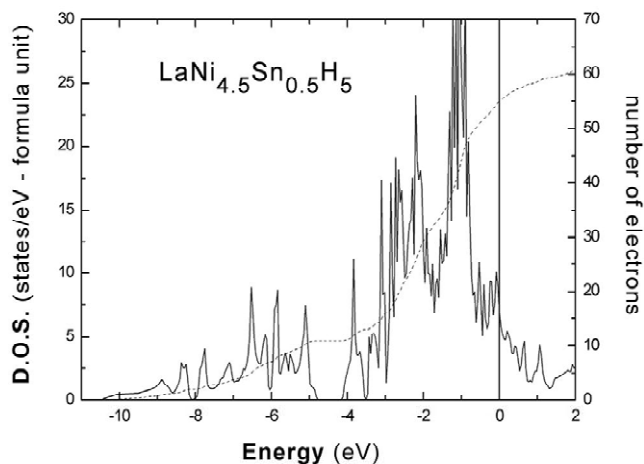


Fig. 6. Total density of states (full line, left hand side scale) and number of electrons (dashed line, right hand side scale) of $\text{LaNi}_{4.5}\text{Sn}_{0.5}\text{H}_5$.

4.2. Electronic structure of the hydride $\text{LaNi}_{4.5}\text{Sn}_{0.5}\text{H}_5$

The DOS of $\text{LaNi}_{4.5}\text{Sn}_{0.5}\text{H}_5$ shown in Fig. 6 is characterised by a broad low energy structure extending from

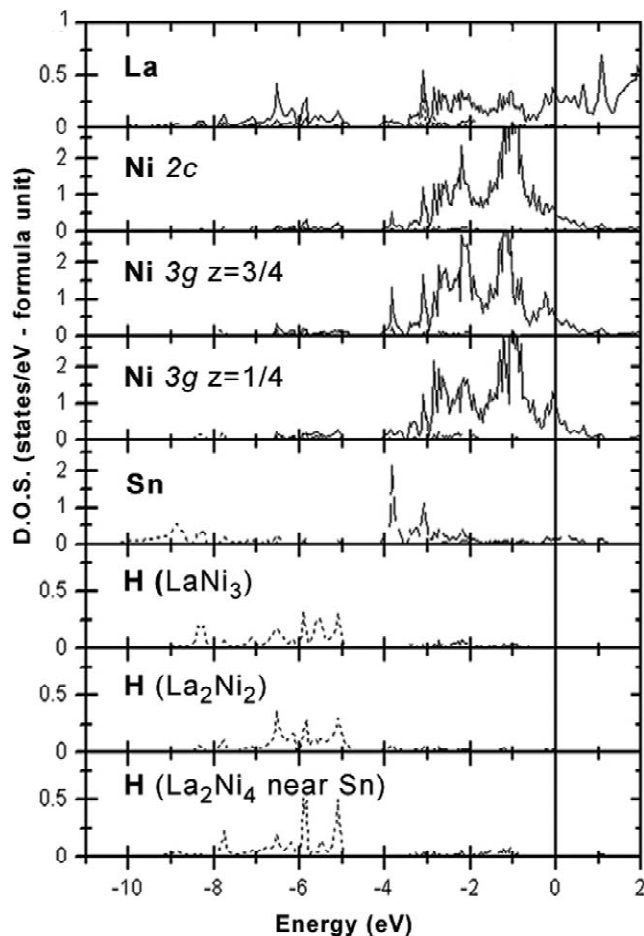


Fig. 7. Partial wave analysis of density of states (DOS) of $\text{LaNi}_{4.5}\text{Sn}_{0.5}\text{H}_5$ around the atomic sites (d states: full line, p states: dashed line, s states: dotted line).

–10.5 to –4.5 eV; it corresponds mostly to the Sn-s states below –8 eV and at higher energies to the five bands associated with metal–hydrogen bonding. The individual contribution of each atom to these bonds is provided by the partial DOS decomposition of Fig. 7. The total contribution of the metal–hydrogen bonding states is dominated by Ni–H interaction, however the extended La-5d orbitals participate also significantly in the metal–hydrogen bonding, it can be seen in Fig. 7 that their contribution per atom is larger than that of the individual Ni-3d, H-s interaction. The 5s states of Sn are broadened in the hydride by the interaction with the H-s states of the first neighbour located at 2.54 Å from Sn.

Above a weak gap of 0.06 eV, the structure around –4 eV is associated to the 5p-states of Sn interacting with the 3d orbitals of the first and second Ni neighbours.

Due to the lattice expansion of the hydride the Ni-d, La-d interaction is weakened, the bands are narrower and the valley separating the bonding and anti-bonding states is smeared out.

In the hydride, the contribution of the Ni-d states at E_F remains higher than that of the La-d states.

The greatest stability of the tin substituted hydride can be essentially ascribed to two factors: (i) the shift of E_F towards higher energies appears to be smaller than in LaNi_5H_5 and (ii) the increased contribution of the low energy metal–hydrogen and metal–tin bonding states.

5. Conclusion

In the substituted intermetallic compounds, the s states of the group IVA element lead to a new low-energy structure in the DOS located around 9 eV below the Fermi level while the p states, located at higher energies interact with the metal-d states. The chemical bonding interactions of Sn with La and Ni found in our calculations can play a role in preventing metal diffusion and improving the cycling lifetime of the intermetallic observed experimentally [9,10].

The substitution of Ni in $\text{LaNi}_{5-x}\text{M}_x$ by the group IVA elements leads to a further filling of the Ni-d bands and to a decrease of the DOS at the Fermi level. The number of holes in the Ni-d bands is more sensitive to the value of x than to the nature of the substituting IVA element. This explains: (i) the decrease of the maximum hydrogen content as x increases and (ii) the fact that for a given value of x , the maximum H absorption capacity is not very sensitive to the nature of the substituting IVA element.

In the corresponding hydrides, the metal–hydrogen interaction leads to the presence of a broad low-energy bonding structure merging with Sn-s states, a factor that contributes to the stability.

The DOS at E_F remains high due to an important contribution of Ni-d states.

We found that the greater stability of the tin substituted

hydride compared to LaNi_5H_5 is due to metal–hydrogen and metal–tin bonding effects as well as to smaller shift of E_F towards higher energies.

Acknowledgements

We would like to thank the IDRIS (Institut de Développement et Recherche en Informatique Scientifique) of the CNRS (Centre National de la Recherche Scientifique) for providing the computing facilities for performing our electronic structure calculations.

References

- [1] H.H. van-Mal, K.H.J. Buschow, A.R. Miedema, *J. Less-Common Met.* 35 (1) (1974) 65.
- [2] M.H. Mendelsohn, D.M. Gruen, A.E. Dwight, *Nature* 269 (5623) (1977) 45.
- [3] A. Percheron-Guégan, C. Lartigue, J.-C. Achard, *J. Less-Common Met.* 104 (1) (1984) 207.
- [4] S. Luo, W. Luo, J.D. Clewley, T.B. Flanagan, L.A. Wade, *J. Alloys Comp.* 231 (1995) 467.
- [5] S. Luo, W. Luo, J.D. Clewley, T.B. Flanagan, R.C. Bowman Jr., *J. Alloys Comp.* 231 (1995) 473.
- [6] C. Witham, R.C. Bowman Jr., B. Fultz, *J. Alloys Comp.* 253–254 (1997) 574.
- [7] R.C. Bowman Jr., C.A. Lindensmith, S. Luo, T.B. Flanagan, T. Vogt, *J. Alloys Comp.* 330–332 (2002) 271.
- [8] S. Luo, T.B. Flanagan, R.C. Bowman Jr., *J. Alloys Comp.* 330–332 (2002) 531.
- [9] R.C. Bowman Jr., C.H. Luo, C.C. Ahn, C.K. Witham, B. Fultz, *J. Alloys Comp.* 217 (1995) 185.
- [10] B.V. Ratnakumar, C.K. Witham, R.C. Bowman Jr., A. Hightower, B. Fultz, *J. Electrochem. Soc.* 143 (1996) 2578.
- [11] M. Gupta, *Int. J. Quantum Chem.* 77 (6) (2000) 982.
- [12] V. Paul-Boncour, M. Gupta, J.-M. Joubert, A. Percheron-Guégan, P. Parent, C. Laffon, *J. Mater. Chem.* 10 (12) (2000) 2741.
- [13] J.-M. Joubert, M. Latroche, R. Černý, R.C. Bowman Jr., A. Percheron-Guégan, K. Yvon, *J. Alloys Comp.* 293–295 (1999) 124.
- [14] J.-C. Achard, A.J. Dianoux, C. Lartigue, A. Percheron-Guégan, F. Tasset, in: *The Rare Earths in Modern Science and Technology*, Vol. 3, Plenum Press, New York, 1982, pp. 481–486.
- [15] J.-M. Joubert, M. Latroche, R.C. Bowman Jr., A. Percheron-Guégan, F. Bourée-Vigneron, *Appl. Phys. A*, submitted.
- [16] M.L. Wasz, P.B. Desch, R.B. Schwarz, *Phil. Mag. A* 74 (1) (1996) 15.
- [17] C. Lartigue, A. Percheron-Guégan, J.-C. Achard, J.-L. Soubeyroux, *J. Less-Common Met.* 113 (1985) 127.
- [18] O.K. Andersen, *Phys. Rev. B* 12 (8) (1975) 3060.
- [19] M. Gupta, *J. Less-Common Met.* 130 (1987) 219.
- [20] M. Gupta, *J. Alloys Comp.* 293–295 (1999) 190.